

# Characterization of Atmospheric Carbonaceous Species in PM<sub>10</sub> over Darjeeling, an Eastern Himalayan Region of India



Akansha Rai, A. Chatterjee, T. K. Mandal, and S. K. Sharma

**Abstract** Carbonaceous aerosol (CAs) pollution is a significant cause of the deterioration of the susceptible Himalayan region, which profoundly affects climate change. In this study, we examined the winter-time pollution load of carbonaceous species [Organic Carbon (OC), Elemental Carbon (EC), Water-Soluble Organic Carbon (WSOC), Water-Soluble Ionic Species (WSIS), Primary Organic Carbon (POC), Secondary Organic Carbon (SOC), and Total Carbonaceous Aerosols (TCAs)] of PM<sub>10</sub> over a semi-urban high-altitude site of Darjeeling (27.041° N, 88.266° E, 2200 m above mean sea level (AMSL); an eastern Himalayan region), India, from January to February 2019. During winter, the PM<sub>10</sub> concentration ( $\mu\text{g m}^{-3}$ ) was found to be  $52 \pm 18$ , which comprises 24% of CAs, 30% of WSIS, and 8% of sea salts. The secondary aerosols contribute about 79% to WSIS and 24% to PM<sub>10</sub>. The average concentration of WSIS was observed in the order of  $\text{SO}_4^{2-} > \text{NH}_4^+ > \text{NO}_3^- > \text{Na}^+ > \text{K}^+ = \text{Ca}^{+2} > \text{Cl}^- > \text{Mg}^{+2} > \text{F}^-$ , respectively. Lower ECR (Effective Carbon Ratio) suggests a reduction in the number of scatterings CAs and possibly an increase in the absorbing CAs. The mean OC/EC ratio ( $2.04 \pm 0.37$ ),  $\text{K}^+/\text{OC}$  ( $0.11 \pm 0.04$ ), and their good correlations of 0.77 and 0.74, respectively, suggested fuel combustion (biomass burning and fossil fuels) as the major contributing source in Eastern Himalayas. In addition, a high WSOC/OC ratio ( $0.74 \pm 0.22$ ) implied the formation of secondary aerosols and the presence of aged aerosols. The trajectory analysis showed that the air masses mainly originated from the IGP region, Nepal, and the local region of the sampling site.

---

A. Rai (✉) · T. K. Mandal · S. K. Sharma  
CSIR-National Physical Laboratory, Dr. K. S. Krishnan Road, New Delhi 110012, India  
e-mail: [akansha.npl19j@acsir.res.in](mailto:akansha.npl19j@acsir.res.in); [akansharai.may@gmail.com](mailto:akansharai.may@gmail.com)

Academy of Scientific and Innovative Research (AcSIR), Ghaziabad 201002, India

T. K. Mandal  
e-mail: [tuhin.npl@nic.in](mailto:tuhin.npl@nic.in)

S. K. Sharma  
e-mail: [sudhir.npl@nic.in](mailto:sudhir.npl@nic.in)

A. Chatterjee  
Environmental Science Section, Bose Institute, Saltlake, Kolkata 700091, India  
e-mail: [abhijit.boseinst@gmail.com](mailto:abhijit.boseinst@gmail.com)

**Keywords** PM<sub>10</sub> · Carbonaceous species · Secondary aerosols · Sources · Darjeeling

## 1 Introduction

Globally, air pollution is the most common environmental contributor to premature death. There are several air pollutants, each with their chemical composition, reaction behaviors, emissions, environmental permanence, capacity to be transported, and eventual influence on the quality of air and human well-being [1, 2]. Due to its detrimental impacts on atmospheric chemistry, quality of air, reduced vision, the Earth's radiation budget, and human health, particulate matter (PM) has a substantial impact [3, 4]. Because they have implications for pollution problems, improvements in our understanding of atmospheric aerosols are an essential study concern [5]. Recently, organic and elemental carbon, denoted as OC and EC, comprises most of the carbonaceous aerosols (CAs) and has received the most attention. EC is a by-product of the partial combustion of fuels (fossil fuels (FFC) and biomass (BB)) from human-made sources [6, 7]. Primary organic carbon (POC) and secondary organic carbon (SOC) are other components of OC. POC is emitted from anthropogenic or biogenic sources. On the other hand, with in-situ reactions of POC, SOC is formed. Water-soluble organic carbon (WSOC) can either come from primary emissions or be created by a chain reaction of organic compounds in the atmosphere while they are transported. It significantly affects hygroscopic characteristics, radiative forcing, and cloud condensation nuclei (CCN) [8–10]. In urbanized climates, water-soluble ionic species (WSIS) constitute a significant fraction of 50–70% mass of PM<sub>2.5</sub> [11]. Additionally, due to their aerosol hygroscopicity, secondary inorganic ions (NO<sub>3</sub><sup>-</sup>, SO<sub>4</sub><sup>2-</sup>, and NH<sub>4</sub><sup>+</sup>), essential components of WSIS, could worsen a decrease in visibility and lead to the formation of a haze [12].

The study of airborne particles over the Himalayan region is of utmost importance since the ecosystem of that region is seriously threatened by various environmental pollutants. Due to high vehicular traffic because of tourists, biomass burning for cooking, and fuelwood burning for heating, play a significant role in loading anthropogenic aerosols over the Himalayan region [13–15]. Due to their relatively longer lifetime (several days to weeks), PM and its species often disperse far from their site of origin [7, 16]. Limited studies were conducted earlier on the physicochemical characterization of aerosols over the eastern Himalayas. They did not enlighten the possible sources of pollutants/aerosols from long-range regions [14, 17]. Thus, it is crucial to examine the pollutant concentrations, chemical characteristics, temporal fluctuations, and the impact of WSIS in the atmosphere over the eastern Himalayas of India.



**Fig. 1** Map of PM<sub>10</sub> sampling site in the Eastern Himalayan region of India (Source Google Earth)

## 2 Site Description

In this study, the sampling was performed at Darjeeling, a well-known hill station over the eastern Himalayas, for tourists. The sampling location is close to the Indo-Gangetic Plain (IGP), located ~50 km with a dense population with substantial aerosol mass loadings. The sampling site was located inside the Bose Institute (27.01° N, 88.15° E) at an altitude of 2200 m above mean sea level (AMSL), as shown in Fig. 1. Around the sample site, and there are numerous tea processing facilities and gardens that occupy 17,500 acres of land [14, 15]. Darjeeling Himalayan Railway (Toy Train) is a world heritage site UN (United Nations) which still runs on coal. The seasonal variations of aerosols produce subsequent signatures on the different physicochemical characteristics of aerosols [7].

## 3 Methodology

### 3.1 Sample Collection

For the collection of PM<sub>10</sub> samples ( $n = 25$ ), a respirable dust sampler (RDS) was used during the sampling period (January–February 2019). On the building's rooftop, 15 m above ground level (AGL), the sampler was placed on the Bose Institute campus. For 24 h, ambient air was filtered through  $20 \times 25 \text{ cm}^2$  PALLFLEX quartz microfibre filters at a flow rate of  $1.2 \text{ m}^3 \text{ min}^{-1}$  (flow accuracy:  $\pm 2\%$ ). The standard protocol was followed for PM<sub>10</sub> sampling using a Sartorius microbalance (resolution:  $\pm 10 \text{ }\mu\text{g}$ ). After the samples were collected, the filters were placed in a deep freezer and stored at a temperature of  $-20 \text{ }^\circ\text{C}$  until analysis.

### 3.2 Chemical Analysis

*OC and EC analysis:* Using an OC/EC carbon analyzer (Model: DRI 2001A, CA, USA), a punch of  $0.536 \text{ cm}^2$  of  $\text{PM}_{10}$  filter was used to determine OC and EC concentrations by following the IMPROVE-A carbon protocol. The thermal-optical analysis is the method-defined for the analyzer based on the successive oxidation of OC and EC at different temperatures. A previous publication has discussed the details regarding the operating procedure, calibration, and calibration standards [7].

*Water-Soluble Organic Carbon (WSOC) analysis:* Using a Shimadzu TOC analyzer, a punch of  $3.79 \text{ cm}^2$  of  $\text{PM}_{10}$  filter was used to determine WSOC concentration. The filter was cut in 20 ml of deionized water (resistivity:  $18.2 \text{ M}\Omega \text{ cm}$ ), sonicated for 30 min and filtered using a nylon membrane. Its working principle is based on catalytic-oxidation combustion of carbonaceous compounds at  $680 \text{ }^\circ\text{C}$ . The details regarding these methods have been discussed elsewhere [7].

*Water-Soluble Ionic Species (WSIS) analysis:* The collected  $\text{PM}_{10}$  samples were analyzed for WSIC using Ion Chromatography (IC Model: Metrohm 930 Compact IC Flex, USA). The left filtered extract (10 ml) from WSOC analysis was used to estimate ionic species. The cations and anions were measured using a 930 Compact IC Flex (Metrohm, Switzerland) system equipped with a Metrosep C4150/4.0 and ASRS-4MN columns, respectively. The details regarding these methods have been discussed in [18].

### 3.3 Air Mass Trajectory Analysis

In the Himalayan region, Hybrid Single-Particle Lagrangian Integrated Trajectory Model (HYSPLIT) trajectory models are crucial for examining the movement of pollutants, long-term passage patterns, and probable local sources of  $\text{PM}_{10}$  [15, 19]. The air parcel back trajectories were downloaded for the sampling days for 500 m AGL. In order to estimate backward trajectories using the isentropic model calculation approach, three days (i.e., 72 h) were chosen because  $\text{PM}_{10}$  can travel a great distance. The geographical area of air parcels approaching a receptor site is created by the backward trajectory analysis, which generates enormous sets of trajectories [4, 20].

*Cluster Analysis:* Using Ward's hierarchical technique, cluster analysis is employed to integrate all air mass trajectories into discrete transport groups arriving at the sampling location. The Euclidean distance was applied to identify the coordinates as variables of the distance between two trajectories and calculated using Eq. 1 to examine the direction of air masses [21, 22]:

$$d_{ij} = \sqrt{\sum_{k=1}^p \left( (x_i(k) - x_j(k))^2 + (y_i(k) - y_j(k))^2 \right)}, \quad (1)$$

where  $p$  denotes the point in  $p$ -dimensional space,  $X_i$  and  $Y_i$  are denoted to the location of trajectory 1.  $X_j$  and  $Y_j$  are denoted to the location of trajectory 2. The ‘eye ball’ method was used to identify the appropriate cluster number by analyzing the disparities between the mean trajectories data [7, 21].

*Concentration Weighted Trajectory (CWT) Method:* The relative importance of probable source locations and their spatial distribution are determined using the CWT approach [15]. To calculate trajectory-weighted concentrations (WCWT), the geographical magnitude of the air mass trajectories determines how the total area occupied by the back trajectories is fragmented into a series of grid cells concerning its pollutant concentrations, as given in Eq. 2 [7, 21, 22]:

$$C_{ij} = \frac{1}{\sum_{k=1}^N \tau_{ijk}} \sum_{k=1}^N c_k \tau_{ijk}, \quad (2)$$

$C_{ij}$  denotes the mean concentration weighted in particular  $(i, j)$ th cell,

$k$  denotes the trajectory’s index,

$N$  represents the overall number of trajectories,

$C_k$  is the pollutant concentration measured during the entry of trajectory  $k$ , and

$\tau_{ijk}$  denotes the time spent in the  $(i, j)$ th cell by trajectory  $k$ .

## 4 Result and Discussion

### 4.1 Mass Concentration of PM<sub>10</sub>

The average winter-time concentration of PM<sub>10</sub> was observed as  $52 \pm 18 \mu\text{g m}^{-3}$  with a range of  $21\text{--}89 \mu\text{g m}^{-3}$  at Darjeeling. Table 1 shows the statistical overview of PM<sub>10</sub> with a 34.5% coefficient of variation during the winter. The monthly average concentration of PM<sub>10</sub> was found to be comparatively lower in the month of January ( $43 \pm 11 \mu\text{g m}^{-3}$ ) and higher in February ( $59 \pm 20 \mu\text{g m}^{-3}$ ). Similar observations were reported by [23] at Pohara ( $51.8 \pm 18.9 \mu\text{g m}^{-3}$ ) in the North-Western Himalayas, [20] at Nainital ( $39 \pm 10 \mu\text{g m}^{-3}$ ), Central Himalayas, [17] at Mohal-Kullu ( $51 \pm 16 \mu\text{g m}^{-3}$ ), Western Himalayas.

**Table 1** PM<sub>10</sub> statistical overview

Number of samples ( <i>n</i> )	25
Average concentration ( $\mu\text{g m}^{-3}$ )	52
Standard deviation	18
Standard error	4
Median ( $\mu\text{g m}^{-3}$ )	50
Range ( $\mu\text{g m}^{-3}$ )	21–89
Minimum concentration ( $\mu\text{g m}^{-3}$ )	21
Maximum concentration ( $\mu\text{g m}^{-3}$ )	89
Confidence level (95%)	7
Coefficient of variation (%)	34.5

#### 4.2 Carbonaceous Species (OC, EC, and WSOC) and Effective Carbon Ratio (ECR) in PM<sub>10</sub>

The average winter-time concentrations of carbonaceous species (OC, EC, POC, SOC, TCAs, and WSOC) of PM<sub>10</sub> with maxima, minima, and median are summarized in Table 2. High concentration of OC ( $5.4 \pm 2.0 \mu\text{g m}^{-3}$ ), EC ( $2.7 \pm 1.0 \mu\text{g m}^{-3}$ ), and WSOC ( $3.8 \pm 1.3 \mu\text{g m}^{-3}$ ) was observed (in Fig. 2), which ranges from 2.1–12.3  $\mu\text{g m}^{-3}$ , 1.4–5.3  $\mu\text{g m}^{-3}$ , and 0.2–7.5  $\mu\text{g m}^{-3}$ , respectively that might be due to local burning activities during the study period. The average concentration of carbonaceous aerosols (TCAs = OC  $\times$  1.6 + EC) was  $11.4 \pm 4.1 \mu\text{g m}^{-3}$  and contributed around ~22% to PM<sub>10</sub>. The POC and SOC were also computed using the EC tracer approach, which contributes 35 and 65% to OC, whereas WSOC contributes 70% to OC. The higher fraction of WSOC in the total OC indicated the aged nature of the carbonaceous aerosols. The substantial concentrations of CAs could be attributed to the enhanced impact of firewood burning for space heating, steady meteorological conditions, and open burning that led to the deposition of pollutants in the lower atmosphere.

The effective carbon ratio (ECR) indicates a link between CAs and climate change, taking into account the absorption properties of POC, which can be calculated as:  $\text{ECR} = \text{SOC}/\text{POC} + \text{EC}$ . The average winter-time ECR was estimated as  $0.32 \pm 0.16$ , which varied from 0.01 to 0.6. According to [24], ECR values less than 0.30 indicate low SOC concentrations, implying a decrease in the quantity of scattering CAs and maybe an upsurge in the absorbing type of CAs.

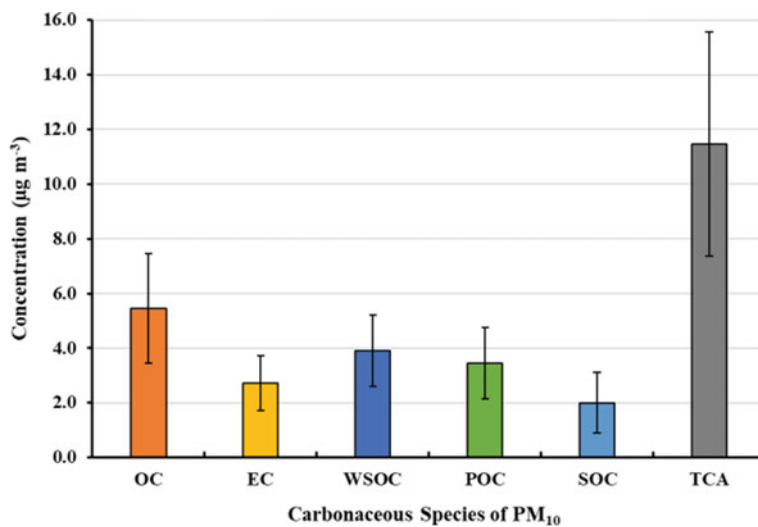
#### 4.3 Waters-Soluble Ionic Species (WSIS) in PM<sub>10</sub>

The average winter-time concentrations of WSIS ( $\text{Na}^+$ ,  $\text{K}^+$ ,  $\text{Mg}^{2+}$ ,  $\text{Ca}^{2+}$ ,  $\text{F}^-$ ,  $\text{Cl}^-$ ,  $\text{NH}_4^+$ ,  $\text{NO}_3^-$  and  $\text{SO}_4^{2-}$ ) of PM<sub>10</sub> with maxima, minima, and median are summarized in Table 2. The average winter sum of WSIS ( $\Sigma\text{WSIS}$ ) concentration ( $15.5 \pm$

**Table 2** Average concentrations of carbonaceous and ionic constituents (in  $\mu\text{g m}^{-3}$ ) of PM<sub>10</sub> at Darjeeling

Species	Average ( $n = 25$ )	Min	Max	Median
OC	$5.4 \pm 2.0$	2.1	12.3	5.1
EC	$2.7 \pm 1.0$	1.4	5.3	2.5
POC	$3.6 \pm 1.3$	1.8	6.9	3.3
SOC	$1.9 \pm 1.1$	0.1	5.4	2.0
TCAs	$11.4 \pm 4.1$	4.7	25.0	10.4
WSOC	$3.8 \pm 1.3$	0.2	7.5	3.9
Na <sup>+</sup>	$1.4 \pm 0.7$	0.1	4.0	1.4
K <sup>+</sup>	$0.6 \pm 0.4$	0.1	1.8	0.6
Mg <sup>2+</sup>	$0.1 \pm 0.1$	0.01	0.5	0.1
Ca <sup>2+</sup>	$0.6 \pm 0.3$	0.1	1.5	0.6
F <sup>-</sup>	$0.04 \pm 0.1$	0.01	0.2	0.02
Cl <sup>-</sup>	$0.4 \pm 0.2$	0.02	0.9	0.3
NH <sub>4</sub> <sup>+</sup>	$4.0 \pm 4.1$	0.3	16.0	3.2
NO <sub>3</sub> <sup>-</sup>	$2.4 \pm 2.5$	0.4	11.7	1.7
SO <sub>4</sub> <sup>2-</sup>	$5.9 \pm 5.2$	0.5	19.7	5.2

± Standard Deviation

**Fig. 2** Mass concentration of carbonaceous species of PM<sub>10</sub>

12.2  $\mu\text{g m}^{-3}$ ) contributed nearly 30% to  $\text{PM}_{10}$ . In terms of concentration,  $\text{SO}_4^{2-}$ ,  $\text{NO}_3^-$ , and  $\text{Cl}^-$  were the most prevalent anions, whereas  $\text{NH}_4^+$ ,  $\text{Na}^+$ , and  $\text{K}^+$  were the most prevalent cations. Based on winter average percentage contribution, the trend of most dominant ions was found to be in the order of  $\text{SO}_4^{2-}$  (38%) >  $\text{NH}_4^+$  (26%) >  $\text{NO}_3^-$  (16%) >  $\text{Na}^+$  (9%) >  $\text{K}^+$  (4%) =  $\text{Ca}^{+2}$  (4%) >  $\text{Cl}^-$  (2%) >  $\text{Mg}^{+2}$  (1%) >  $\text{F}^-$  (0.2%). A marker for secondary inorganic aerosols (SIA) is sulphate-nitrate ammonium (SNA) which contributes around 24% of the  $\text{PM}_{10}$  concentration and 79% to WSIC. Only ~8% of sea salts were reported during the winter season. The charge balance of ionic species showed a good correlation of 0.79, as shown in Fig. 3f.

#### 4.4 Diagnostic Ratios and Scatter Plots

The diagnostic ratios of  $\text{PM}_{10}$  species (OC, EC, SOC, and WSOC) aid in determining the formation and removals processes of secondary organic aerosols (SOA), the aging of atmospheric aerosols, and the emission of CAs (Fig. 3a–c). The ratio of OC/EC suggests the origin of aerosols emitted from various sources, both locally produced and transported. In this study, the ratio of OC/EC ranged from 1.31 to 2.61, with an average of  $2.04 \pm 0.37$  and a good correlation of 0.77. This indicates that fossil fuel combustion (FFC) is influenced mainly by tourist vehicles and local biomass burning (BB), as well as over the IGP region. Aerosols produced by BB and FFC can be identified using the ratios of  $\text{K}^+$  with OC and EC. The ratio of  $\text{K}^+$ /OC varied from 0.04–0.21 for BB and agricultural residue burning, which shows a good correlation of 0.74 (Fig. 3d). Similarly, relatively high  $\text{K}^+$ /EC ratios were recorded for BB with a range of 0.06–0.53 and a significant correlation of 0.52 (Fig. 3e). On the other hand, WSOC/OC ratio can also be used as a tracer for emission sources, strength, and SOA contribution. In the present study, the ratio of WSOC/OC varied from 0.08 to 0.94, with an average ratio of  $0.72 \pm 0.19$  and a significant correlation of 0.66. In the atmosphere, the photochemical oxidation reactions of volatile organic compounds (VOCs) through the gas-phase conversion are generally responsible for the high WSOC/OC ratio, i.e., through SOA formation. The obtained results indicate the emissions from FFC, widespread BB practices, and the production of SOC due to carbonaceous species transported from the surrounding IGP region.

#### 4.5 Air Mass Backward Trajectory

Backward trajectory analysis is a conventional technique for identifying the location, airflow, and transport of aerosols imposing severe pollution load in the Himalayan region [15, 19]. In Fig. 4a, the 500 m trajectories originated from different regions in Nepal, the north-western regions of India, the Thar desert, central highlands, the semi-arid region, the IGP region, and Bhutan, demonstrating that the near-surface flows are chaotic in nature [7]. The medium-range transport was observed with heavy



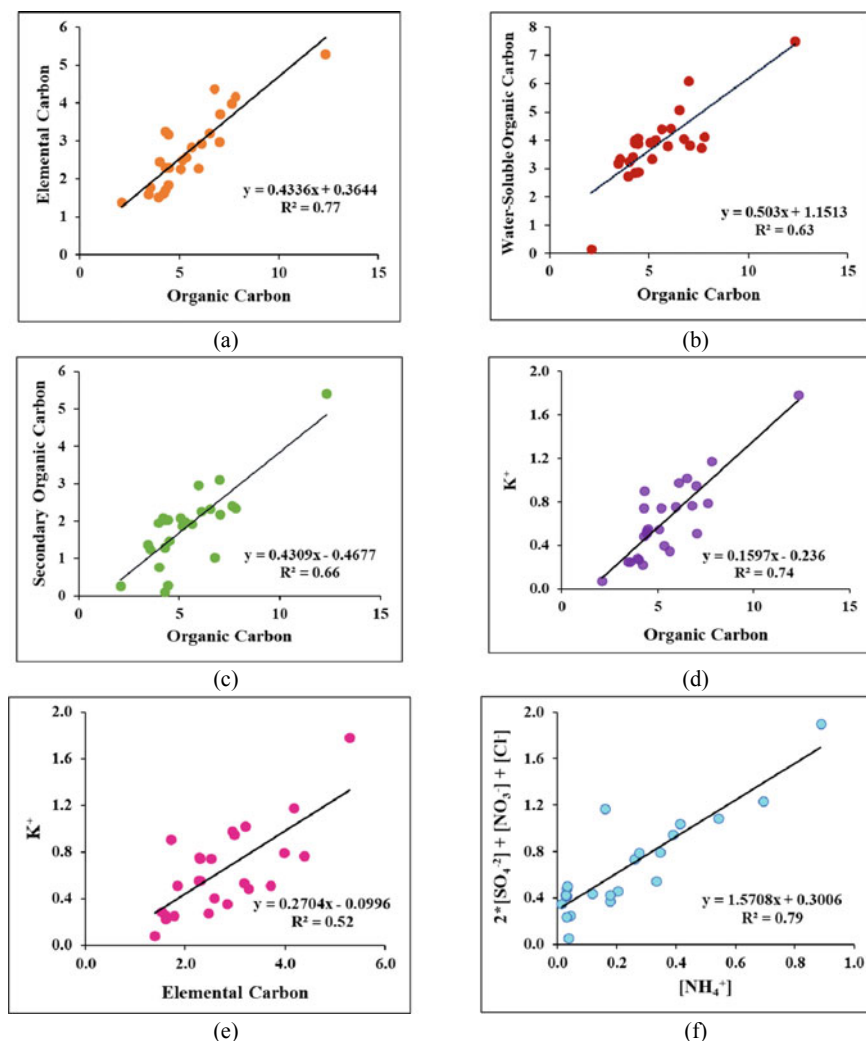


**Fig. 3** Scatter plots of species of PM<sub>10</sub> **a** OC with EC **b** OC with WSOC **c** OC with SOC **d**  $K^+$  with OC **e**  $K^+$  with EC **f** ionic charge balance

air mass loading at the IGP region. Whereas the long-distant passage of pollutants was observed from the north-western region, passing over China and approaching the receptor site.

*Cluster Analysis of PM<sub>10</sub>*: Cluster analysis was performed at an altitude of 500 m AGL to limit the impacts of surface friction and to simulate breezes in the lower boundary layer. The trajectory numbers of trajectories after clustering from different directions are depicted in Fig. 4b. Cluster 1 (orange color) belongs to short-range transport,

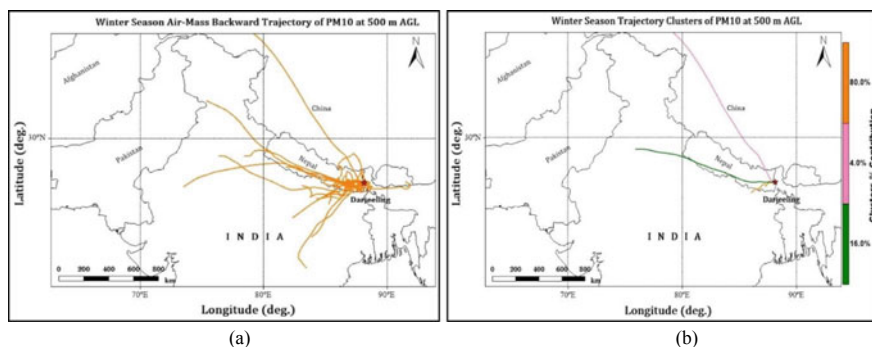


**Fig. 4** Air-mass backward trajectory (a) and cluster analysis (b) of PM<sub>10</sub> during the winter season at 500 m AGL over Darjeeling

which accounts for 80% of air mass trajectory originating from the local and lowers IGP region, which is the most polluted belt in India. Cluster 2 (green color) belongs to medium-range transport, which accounts for 16% of air mass trajectory originating from the Thar desert and passing through Nepal and the IGP region towards the receptor site. In contrast, cluster 3 (pink colour) represented the long-distant passage of air masses (accounting for 4% of the total) from the north-western pathway passing over China. The short-distant trajectories were observed to correspond to the slow-moving parcel of air masses. On the other hand, highly long pathways indicate strong flows, which significantly impact the quality of the atmosphere differently [15, 25].

*CWT Analysis of PM<sub>10</sub> along with its species (OC, EC, TCA, POC, SOC, WSOC, SIA):* The WCWT were applied to identify the influence of the probable sources by aggregating apportionment numbers for each source and evaluating the pollution level associated with various trajectories. In Fig. 5a, the local area, lower IGP region, and Nepal contribute to higher concentration (WCWT values) of PM<sub>10</sub>, and low concentration was observed in the IGP region of India. From the observed results of winter-time PM<sub>10</sub> and its carbonaceous species, it was found that these species might be generated by incomplete burning of fuel and wood at low temperatures, which are employed to combat chill—owing to the trapping of coarse particulates in the fog and calm breeze, a persistent thermal inversion with constrained dispersion forms at ground level.

The higher concentration of OC (Fig. 5b) and reconstructed POC (Fig. 5d) was observed in local and Nepal regions, which may contribute to fungal spores, plant debris, and biomass burning activities. The long-distant pathway of TCA through the prevailing westerly wind was assessed over Nepal, and local areas (Fig. 5e). Whereas EC (Fig. 5c) and SIA (Fig. 5g) concentrations were increased from the IGP region to Nepal and near the receptor site, which might contribute to the emissions from the vehicular exhaust and secondary aerosols. Higher concentrations of SOC (Fig. 5f) and WSOC (Fig. 5h) over the sampling area and Nepal region showed the emissions from the secondary aerosol formation, as reported by [10].

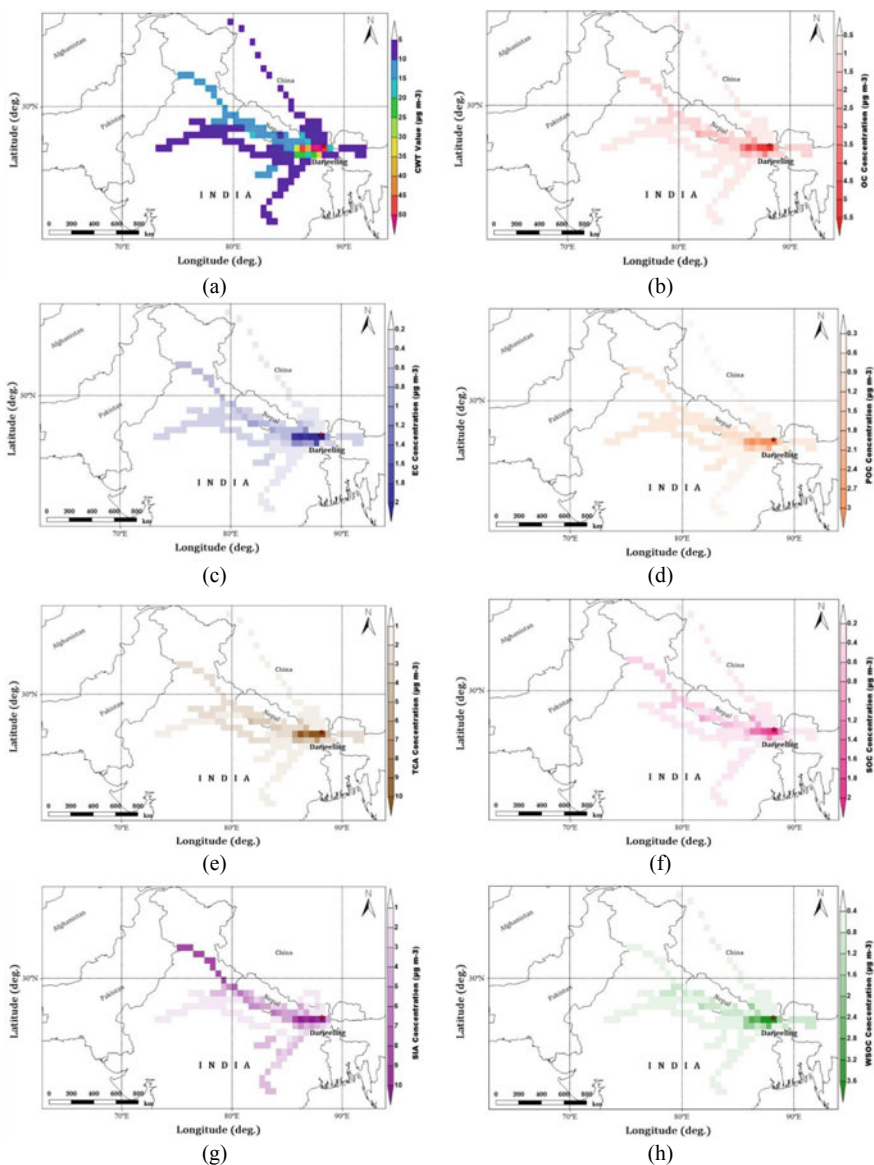


**Fig. 5** CWT plots of **a** PM<sub>10</sub>, **b** OC, **c** EC, **d** POC, **e** TCA, **f** SOC, **g** SIA, **h** WSOC ( $\mu\text{g m}^{-3}$ ) during the winter season at 500 m AGL over Darjeeling

Similar results were also observed by [26, 27] in Nainital and Dhulikhel (Nepal), which showed that the accumulation of IGP aerosols and polluted continental air mass consisting of dust and smoke was prevalent during the winter seasons. [28] reported on the complexities of OC sources such as burning, pollen, tiny soil minerals, and mechanisms of secondary organic compounds. Because the pollutants from the suburban areas cannot reach the mountaintop during the winter, the boundary layer stays below Darjeeling (2.2 km), and the atmosphere remains relatively pristine [14]. So, in the winter, there are also fewer human activities involving tourists, which contributes to the local production of CAs.

## 5 Conclusion

The winter-time aerosols of  $PM_{10}$  have been studied at a high-altitude site (Darjeeling) in the eastern Himalayan region of India. The mean concentration ( $\mu\text{g m}^{-3}$ ) of winter-time  $PM_{10}$  was  $52 \pm 18$ , close to NAAQS and WHO limits.

- In this study, the winter-time concentrations ( $\mu\text{g m}^{-3}$ ) of OC ( $5.4 \pm 2.0$ ), EC ( $2.7 \pm 1.0$ ), and WSOC ( $3.8 \pm 1.3$ ) were observed due to the increasing influence of burning wood for domestic purposes, outdoor BB, and steady air conditions.
- WSOC contributes 70% to OC, indicating the aging nature of the CAs. The average winter-time concentration ( $\mu\text{g m}^{-3}$ ) of CAs was  $11.4 \pm 4.1$ , contributing around ~22% to  $PM_{10}$ .
- A lower effective carbon ratio (0.32) suggests a reduction in the number of scatterings CAs and possibly an increase in the absorbing CAs.
- The average winter-time concentration ( $\mu\text{g m}^{-3}$ ) of WSIC was observed as  $15.5 \pm 12.2$ , contributing nearly 30% to  $PM_{10}$ . SIA contributes around 24% of the  $PM_{10}$  concentration and 79% to WSIC.
- A major effect of BB, FFC, and SA as an origin of carbonaceous species over the eastern Himalayan region was revealed by the diagnostic ratios and linear regression analysis of OC with EC, WSOC with OC,  $K^+$  with OC, and EC. These variables were also positively correlated with carbonaceous components.

Based on cluster analysis, 80% of air mass was short-range (local and lower IGP region), 16% was medium-range transport (the Thar desert and passing through Nepal and the IGP region), and 4% was long-range transport of air masses (north-western route passing over China). CWT analysis showed that carbonaceous species traveled from Nepal and the IGP region apart from local emissions.

The present study showed a significant implication for the Himalayan region because the deposition of CAs over Darjeeling, a high-altitude location, is a matter of concern from the human well-being perspective and fragile ecology across the Indian Himalayas. Therefore, it is crucial to reduce the key contributors to  $PM_{10}$  and CAs over the Himalayan region (automobile pollution, FFC, and BB) by implementing effective and efficient waste management techniques, etc. Therefore, this study can

aid the stakeholders and policymakers in understanding the characteristics of PM<sub>10</sub> for the Himalayan region.

**Acknowledgements** The authors are thankful to the Director, CSIR-NPL, New Delhi, for providing their valuable support in carrying out this research work. One of the authors (Akansha Rai) is thankful to the University Grants Commission (UGC) for providing the fellowship. The authors also thank Mrs. Yashodhara Yadav, Bose Institute, Darjeeling, for PM<sub>10</sub> sampling and for providing relevant data sets. The authors also acknowledge the Department of Science and Technology, New Delhi, for providing financial support for this study (DST/CCP/Aerosol/88/2017). Finally, the authors thankfully acknowledge the NOAA Air Resources Laboratory for downloading the air mass trajectories.

## References

1. Akasha H, Ghaffarpasand O, Pope F (2021) Climate change and air pollution. K4D helpdesk report
2. Marina-Montes C, Pérez-Arribas LV, Anzano J, Cáceres JO (2020) Local and remote sources of airborne suspended particulate matter in the antarctic region. *Atmosphere* 11(4):373
3. Buchunde P, Safai PD, Mukherjee S, Leena PP, Singh D, Meena GS, Pandithurai G (2019) Characterization of particulate matter at a high-altitude site in southwest India: impact of dust episodes. *J Earth Syst Sci* 128(8):237
4. Sharma SK, Mandal TK (2017) Chemical composition of fine mode particulate matter (PM<sub>2.5</sub>) in an urban area of Delhi, India and its source apportionment. *Urban Clim* 21:106–122
5. Moretti S, Salmatonidis A, Querol X, Tassone A, Andreoli V, Bencardino M, Naccarato A (2020) Contribution of volcanic and fumarolic emission to the aerosol in marine atmosphere in the central Mediterranean sea: results from Med-Oceanor 2017 cruise campaign. *Atmosphere* 11(2):149
6. Kontuľ I, Kaizer J, Jeřkovský M, Steier P, Povinec PP (2020) Radiocarbon analysis of carbonaceous aerosols in Bratislava, Slovakia. *J Environ Radioact* 218:106221
7. Rai A, Mukherjee S, Choudhary N, Ghosh A, Chatterjee A, Mandal TK, Kotnala RK (2021) Seasonal transport pathway and sources of carbonaceous aerosols at an urban site of eastern Himalaya. *Aerosol Sci Eng* 5(3):318–343
8. Dinoi A, Cesari D, Marinoni A, Bonasoni P, Riccio A, Chianese E, Tirimberio G, Naccarato A, Sprovieri F, Andreoli V, Moretti S, Gulli D, Calidonna CR, Ammascato I, Contini D (2017) Intercomparison of carbon content in PM<sub>2.5</sub> and PM<sub>10</sub> collected at five measurement sites in southern Italy. *Atmosphere* 8(12):243
9. Panicker AS, Kumar VA, Raju MP, Pandithurai G, Safai PD, Beig G, Das S (2021) CCN activation of carbonaceous aerosols from different combustion emissions sources: a laboratory study. *Atmos Res* 248:105252
10. Jin Y, Yan C, Sullivan AP, Liu Y, Wang X, Dong H, Chen S, Zeng L, Collett JL Jr, Zheng M (2020) Significant contribution of primary sources to water-soluble organic carbon during Spring in Beijing, China. *Atmosphere* 11(4):395
11. Bamotra S, Kaushal D, Yadav S, Tandon A (2022) Variations in the concentration, source activity, and atmospheric processing of PM<sub>2.5</sub>-associated water-soluble ionic species over Jammu, India. *Environ Monit Assess* 194(9):1–18
12. Zhao X, Huang Y, Han F, Touseef B, Song Z, Zhao X, Bandna B (2022) The seasonal characterization and source analysis of water-soluble inorganic ions in PM<sub>2.5</sub> in Fuxin, northeast China. *Environ Forensics* 1–12
13. Adak A, Chatterjee A, Singh AK, Sarkar C, Ghosh S, Raha S (2013) Atmospheric fine mode particulates at eastern Himalaya, India: role of meteorology, long-range transport, and local anthropogenic sources. *Aerosol Air Qual Res* 14(1):440–450

14. Sarkar C, Roy A, Chatterjee A, Ghosh SK, Raha S (2019) Factors controlling the long-term (2009–2015) trend of PM<sub>2.5</sub> and black carbon aerosols at eastern Himalaya, India. *Sci Total Environ* 656:280–296
15. Rai A, Mukherjee S, Chatterjee A, Choudhary N, Kotnala G, Mandal TK, Sharma SK (2020) Seasonal variation of OC, EC, and WSOC of PM<sub>10</sub> and their CWT analysis over the eastern Himalaya. *Aerosol Sci Eng* 4(1):26–40
16. Joshi H, Naja M, Gupta T (2020) In-situ measurements of aerosols from the high-altitude location in the Central Himalayas. In: *Measurement, analysis, and remediation of environmental pollutants*. Springer, Singapore, pp 59–89
17. Choudhary N, Srivastava P, Dutta M, Mukherjee S, Rai A, Kuniyal JC, Sharma SK. Seasonal characteristics, sources and pollution pathways of PM<sub>10</sub> at high altitudes Himalayas of India. *Aerosol Air Qual Res* 22:220092
18. Ahmed M, Bhuyan P, Sarkar S, Hoque RR (2022) Seven-year study of monsoonal rainwater chemistry over the mid-Brahmaputra plain, India: assessment of trends and source regions of soluble ions. *Environ Sci Pollut Res* 29(17):25276–25295
19. Kulshrestha U, Kumar B (2014) Airmass trajectories and long-range transport of pollutants: a review of wet deposition scenario in South Asia. *Adv Meteorol*
20. Sharma SK, Choudhary N, Kotnala G, Das D, Mukherjee S, Ghosh A, Mandal TK (2020) Winter-time carbonaceous species and trace metals in PM<sub>10</sub> in Darjeeling: a high altitude town in the eastern Himalayas. *Urban Clim* 34:100668
21. Chen Y, Xie S, Luo B (2018) Seasonal variations of transport pathways and potential sources of PM<sub>2.5</sub> in Chengdu, China (2012–2013). *Front Environ Sci Eng* 12(1):12
22. Li Y, Zhao W, Fu J, Liu Z, Li C, Zhang J, He C, Wang K (2020) Joint governance regions and major prevention periods of PM<sub>2.5</sub> pollution in China based on wavelet analysis and concentration—weighted trajectory. *Sustainability* 12(5):2019
23. Kaushal D, Kumar A, Yadav S, Tandon A, Attri AK (2018) Winter-time carbonaceous aerosols over the Dhauladhar region of North-Western Himalayas. *Environ Sci Pollut Res* 25(8):8044–8056
24. Ramírez O, de la Campa AS, de la Rosa J (2018) Characteristics and temporal variations of organic and elemental carbon aerosols in a high-altitude, tropical Latin American megacity. *Atmos Res* 210:110–122
25. Yang W, Wang G, Bi C (2017) Analysis of long-range transport effects on PM<sub>2.5</sub> during a short severe haze in Beijing, China. *Aerosol Air Qual Res* 17:1610–1622
26. Dumka UC, Kaskaoutis DG (2014) In-situ measurements of aerosol properties and estimates of radiative forcing efficiency over Gangetic-Himalayan region during the GVAX field campaign. *Atmos Environ* 94:96–105
27. Tripathee L, Kang S, Chen P, Bhattarai H, Guo J, Shrestha KL, Sharma CM, Ghimire PS, Huang J (2021) Water-soluble organic and inorganic nitrogen in ambient aerosols over the Himalayan middle hills: seasonality, sources, and transport pathways. *Atmos Res* 250:105376
28. Li C, Yan F, Kang S, Yan C, Hu Z, Chen P, Gao S, Zhang C, He C, Kaspari S, Stubbins A (2020) Carbonaceous matter in the atmosphere and glaciers of the Himalayas and the Tibetan plateau: an investigative review. *Environ Int* 146:106281